Oligo(thienylene ethynylene)s: A New Class of Oligomeric Model Compounds

Peter Bäuerle[†] and Jens Cremer*[,‡]

Department of Organic Chemistry II (Institute of Organic Chemistry II and Advanced Materials), University of Ulm, Albert-Einstein-Allee 11, 89081 Ulm, Germany, and Consortium für elektrochemische Industrie, Wacker Chemie AG, Zielstattstrasse 20, 81379 Munich, Germany

Received December 18, 2007. Revised Manuscript Received January 31, 2008

A series of ethynylene-containing oligothiophenes as new model compounds is reported here. Based on palladium-catalyzed cross-coupling reactions this oligomeric series has been synthesized from a monomer to a tetramer. Their optical and electrochemical properties have been characterized and compared to a structurally related series of oligo(3-hexylthiophene)s, which gives excellent insight into common and deviating physical properties between these two oligomer series. Furthermore, the data analysis provides an insight into the corresponding defectless, infinite polymer chain and gives information about the "effective" conjugation length of the parent real polymer.

Introduction

In a previous work the properties of a new class of polymers and the corresponding polymer−fullerene solar cells have been described.[1] The polymers used therein were poly(3-hexylthiophene) derivatives bearing triple bonds in the polymer backbone which strongly influenced the electronic properties of these materials. In particular the thoroughly investigated poly(hexylbithienylene ethynylene) showed high oxidation potentials making this type of polymer a promising candiate for the use in polymer−fullerene solar cells, and as a result the corresponding photovoltaic devices were characterized by unexpected open-circuit voltages larger than 1 V.

Besides the synthesis and the overall properties of theses polymers, it is of great interest to derive clear structure/property relationships, which however is rather difficult in the case of polymers because their physical properties cannot be directly correlated to their structural parameters. This is mainly due to their character exhibiting a statistical chain length distribution and interruption of the conjugated chain by mislinkages or other defects which will disturb the conjugation and conducting pathways.

Hence, the synthesis and investigation of well-defined model oligomers has become useful to gain insight into the structural and electronic peculiarities of the corresponding polymers. These oligomeric model compounds are superior to their polymeric counterparts with respect to monodisperse chain length and the lack of defects, hindering full conjugation. However, these advantageous properties of the model oligomers are accompanied by the necessity of long well planned and resource demanding synthetic strategies. Nevertheless, a homologous series of defined oligomers of nearly all basic conducting polymers have been synthesized during the last years. The painstaking characterization of these homologous series could be well correlated to the conjugated chain length, resulting in vital information about the mean conjugation length of the corresponding polymer. Furthermore, an extrapolation of the data obtained from optical and electrochemical measurements revealed the character of a hypothetical polymer with an infinite chain length and the lack of all possible occurring defects.[2] It has been shown theoretically[3] and experimentally[2,4] that the electronic properties of conjugated systems are dependent on the chain length and can be found by linear correlation of the properties versus the inverse chain length. Such linear relationships have been demonstrated for homologous oligomer series of various important polymers[2] such as oligo(phenylene)s,[5] oligo(phenylene vinylene)s (OPV),[6] oligo(phenylene ethynylene)s (OPE),[7] oligo(thienylene vinylene)s (OTV),[8] oligo(3-hexylthiophene) (O3HT),[9] and those including combinations of different monomeric units[10,11] have been described in detail. However, this linear behavior is only valid for small oligomer units because beyond this limit a beginning saturation of the electronic properties is typically observed, and consequently, the effective conjugation deviates from the expected linear

* Corresponding author. E-mail: jens.cremer@wacker.com.
[†] University of Ulm.
[‡] Wacker Chemie AG.

(1) Cremer, J.; Wienk, M. M.; Janssen, R. A. J.; Bäuerle, P. *Chem. Mater.* **2006**, *18*, 5832.
(2) Müllen, K.; Wegner, G. *Electronic Materials: The Oligomeric Approach*; Wiley-VCH: Weinheim, 1998.
(3) Diaz, A. F.; Crowley, J.; Bargon, J.; Gardini, G. P.; Torrance, J. B. *J. Electroanal. Chem.* **1981**, *121*, 355.
(4) Lahti, P. M.; Obrzut, J.; Karasz, F. E. *Macromolecules* **1987**, *20*, 2023.
(5) Matsunoka, S.; Fujii, H.; Yamada, T.; Pac, C.; Ishida, A.; Takamuku, M.; Nakashima, N.; Kanagida, S.; Hashimoto, Y.; Sakata, T. *J. Phys. Chem.* **1991**, *95*, 5802.
(6) Meier, H.; Ickenroth, D. *Eur. J. Org. Chem.* **2002**, 1745.
(7) Ickenroth, D.; Weissmann, S.; Rumpf, N.; Meier, H. *Eur. J. Org. Chem.* **2002**, 2808.
(8) Roncali, J. *Acc. Chem. Res.* **2000**, *33*, 147.
(9) Kirschbaum, T.; Azumi, R.; Mena-Osteritz, E.; Bäuerle, P. *New J. Chem.* **1999**, 241.
(10) Liu, L.; Liu, Z.; Xu, W.; Xu, H.; Zhang, D; Zhu, D *Tetrahedron* **2005**, *61*, 3813.
(11) Dahlmann, U.; Neidlein, R. *Helv. Chim. Acta* **1996**, *79*, 755.

10.1021/cm703606h CCC: $40.75
Published on Web 03/20/2008

dependence.[8,12] However, this divergence from the expected linear behavior depends on the chemical structure of the organic semiconductor and in the case of highly confining systems such as OPEs[7,12] occurs very soon after around 4–5 repeating units while for highly delocalized systems, for example, OTVs,[8] the effects cannot be observed for oligomers smaller than 15–20 units.

The abovementioned deviation from linearity originates from mainly two effects. First, an out-of-plane twist of the monomer units leads a deviation from planarity of the polymer backbone. This results in a reduced overlap of the corresponding π-orbitals leading to a containment of the effective conjugation. The out-of-plane twist may be caused due to sterical interactions between the momomeric units or rotations around single bonds.[13,14] Second, the incorporation of aromatic rings into the polymer backbone leads to a preferred localization of the π-electrons which further reduces the effective conjugation. An extrapolation of the electronic properties of the corresponding oligomers to an infinite conjugated chain gives vital information about the effective conjugation length of the parent polymer and allows the estimation of the average chain length of the parent polymers.

Herein, we report on the synthesis of a homologous series of well-defined oligomers **2**, **7**, **9**, and **10**. However, the longest representative of this series, tetramer **10**, is lacking the terminal silyl-protected triple bond. Nevertheless, this small structural deviation does not show a significant influence on the overall electronic properties as concluded from structure–property relationships. The optical and electrochemical properties of this oligomeric series are determined and compared to an analogous series of oligo(3-hexylthiophene)s which have been synthesized prior to this work.[9]

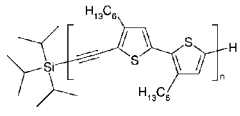

n = 1-3: **2, 7, 9**

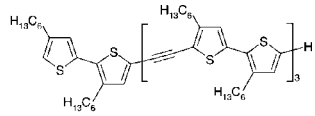

10

Synthesis

The synthesis of the oligomeric model compounds **2**, **7**, **9**, and **10** started from bromo-bithiophene **1**[15] which was converted into the iodine-containing TIPS-protected acetylene **3** and the benzyloxy-protected bithiophene **6**.

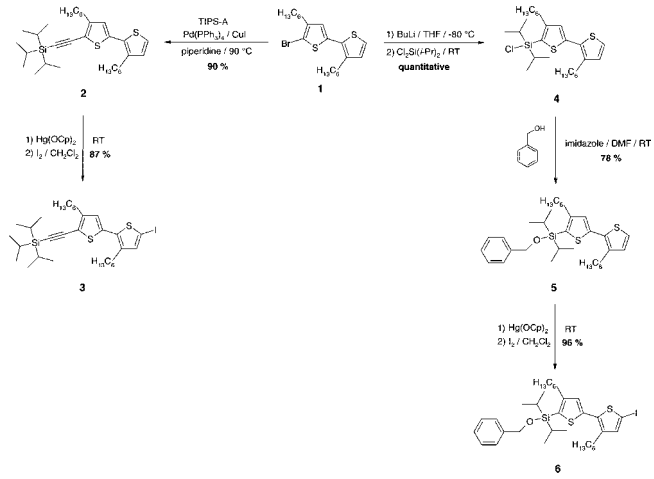

In the first route, acetylenic bithiophene **2** was synthesized starting from bithiophene **1** in a Sonogashira reaction with 1.2 equiv of TIPS−acetylene, 10 mol % cuprous iodide, and 5 mol % $Pd(PPh_3)_4$ in piperidine at 90 °C to give TIPS-protected bithiophene **2** in 90% yield after chromatographic workup. In order to introduce an iodine atom at the reactive α-position of bithiophene **2**, a mercury mediated method was utilized.[16] First, by reacting bithiophene **2** with an equimolar amount of mercury caproate in dry dichloromethane at room temperature, and second, by subsequent addition of 1.1 equiv of iodine, iodinated compound **3** was accessible in 87% yield after column chromatography.

In the second route, bithiophene **1** was converted into chloro-silylated bithiophene **4** by a one-pot, two-step synthesis. First, a bromine−lithium exchange was achieved in THF at −80 °C with 1.02 equiv of *n*-BuLi. The lithiated intermediate was subsequently reacted with 1.5 equiv of dichloro-diisopropyl-silan to give chloro-silylated compound **4** in quantitative yield at room temperature. Immediately, the moisture sensitive bithiophene **4** was converted into the benzyloxy-protected bithiophene **5** by treatment with 1.5 equiv of benzylic alcohol in dry DMF and 3 equiv of imidazole. After stirring the reaction mixture at room temperature for 24 h bithiophene **5** was accessible in 78% yield after column chromatography. Using the mercury mediated method, bithiophene **5** was converted into the iodo-bithiophene **6** in 96% yield after filtration over basic aluminum oxide by reacting **5** with an equimolar amount of mercury caproate in dry dichloromethane at room temperature and subsequent addition of 1.1 equiv of iodine.

Dimer **7** was accessible in 82% yield after column chromatography, when bithiophene **3** was cross-coupled with deprotected ethynylated bithiophene **2a** in a Sonogashira reaction with 5 mol % $Pd(PPh_3)_2Cl_2$ in piperidine at 60 °C for 1 h in the presence of 10 mol % cuprous iodide. For elongation, an iodine functionality was introduced at the free α-position of the terminal bithiophene moiety **7** by first reacting oligomer **17** with an equimolar amount of mercury acetate in dry chloroform at room temperature and subsequent addition of 1.1 equiv of iodine. Iodinated dimer **8** was obtained in 81% yield after column chromatography. To further enhance the conjugated system oligomer **8** was reacted in a subsequent Sonogashira reaction with 1.2 equiv of unprotected acetylene bithiophene **2a**. In analogy to the

(12) Meier, H.; Stalmach, U.; Kolshorn, H. *Acta Polym.* **1997**, *48*, 379.
(13) Roncali, J. *Chem. Rev.* **1997**, *97*, 173.
(14) Jestin, I.; Frère, P.; Blanchard, P.; Roncali, J. *Angew. Chem.* **1998**, *110*, 990.
(15) Cremer, J.; Mena-Osteritz, E.; Pschierer, N. G.; Müllen, K.; Bäuerle, P *Org. Biomol. Chem.* **2005**, *3*, 85.
(16) Kirschbaum, T.; Briehn, C. A.; Bäuerle, P. *J. Chem. Soc., Perkin Trans. 1,* **2000**, 1211.
(17) Hamai, S.; Hirayama, F. *J. Phys. Chem.* **1983**, *87*, 83.
(18) Kirschbaum, T. Dissertation, Ulm University, 2001.
(19) Li, H.; Powell, D. R.; Hayashi, R. K.; West, R. *Macromolecules* **1998**, *31*, 52.

synthesis of dimer **7**, the same reaction conditions have been applied for this palladium-catalyzed cross-coupling, yielding trimer **9** in 45% yield after chromatographic workup. Prior to the last step of this sequence, silyl-protected trimer **9** was reacted with 5 equiv of cesium fluoride in a THF/methanol mixture at 70 °C for 2 h. In this manner, deprotected trimer **9a** was obtained in quantitative yield. Finally, trimer **9a** underwent a Sonogashira reaction with 1.2 equiv of iodinated bithiophene **6**. The cross-coupling reaction has been run in piperidine with 5 mol % $Pd(PPh_3)_4$ and 10 mol % cuprous iodide at 60 °C for 1 h. After the reaction was completed, the intermediate product was desilylated in situ by adding 5 equiv Bu_4NF to the reaction mixture. After stirring at 80 °C for another hour the reaction mixture was worked-up, yielding tetramer **10** in 62% yield after column chromatography.

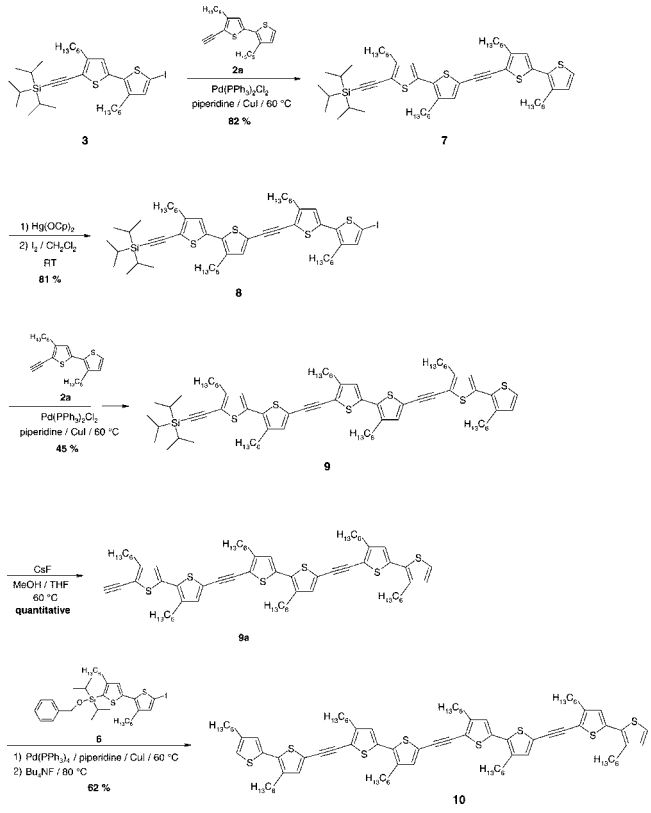

Physical Properties

Absorption and emission spectra of the oligomeric model compound series **2**, **7**, **9**, and **10** depicted in Figure 1 have been measured in chloroform. The corresponding optical properties are given in Table 1.

The spectra reveal a progressive bathochromic shift of the absorption maxima with increasing chain length of the conjugated system. While ethynylated bithiophene **2** shows a maximum at 333 nm, 392 nm is found for the next higher homologue, dimer **7**. Further elongation of the conjugated chain in trimer **9** leads to a progressive red-shift to 417 nm, whereas for tetramer **10** a maximum is found at 427 nm. A similar trend can be seen for the optical band gap which is largest for **2** ($\Delta E_{opt.}$ = 3.21 eV) and decreases steadily with increasing chain length ($\Delta E_{opt.}$ (**10**) = 2.46 eV). It can be concluded from the absorption spectra that the "effective" conjugation is about to approach saturation, and consequently further elongation of the conjugated chain will not significantly alter the optical properties.

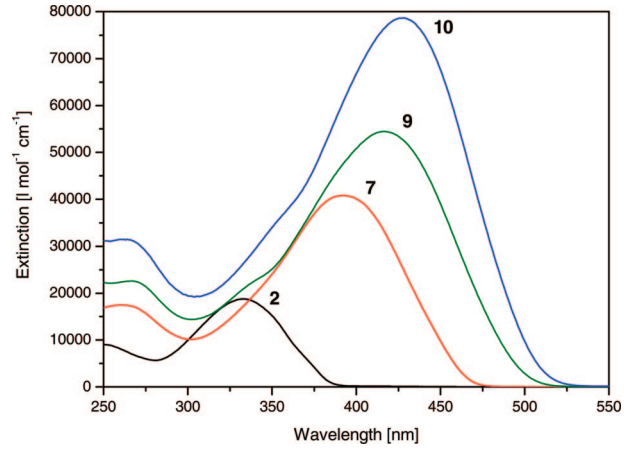

Figure 1. UV–vis spectra of the oligomeric model compounds **2**, **7**, **9**, and **10** in chloroform.

In this respect, the extinction coefficients are gradually enhanced in steps of about 20 000 $mol \cdot L^{-1} \cdot cm^{-1}$ which is almost equal to ε of ethynylated bithiophene **2** (ε = 18 800 $mol \cdot L^{-1} \cdot cm^{-1}$). While the next higher homologue **7** exhibits a coefficient twice as large (ε = 40 800 $mol \cdot L^{-1} \cdot cm^{-1}$) the molar extinction coefficient of the longest homologue **10** is increased by almost a factor of 4 (ε = 78700 $mol \cdot L^{-1} \cdot cm^{-1}$). For comparison the absorption maximum of the parent poly(hexylbithienylene ethynylene) exhibits a value of 451 nm with an optical band gap of $\Delta E_{opt.}$ = 2.35 eV.[1]

The emission maxima of the oligomeric model compounds **2**, **7**, **9**, and **10** are gradually red-shifted with increasing length of the conjugated backbone (Figure 2). While ethynylated bithiophene **2** shows a maximum emission at 410 nm this is steadily shifted to longer wavelengths for the next higher homologues **7** (λ_{max} = 469 nm) and **9** (λ_{max} = 510), finally reaching an emission maximum of 521 nm for tetramer **10**. As typically observed for all oligomeric series, the difference of the emission maxima between the corresponding representatives of this series ($\Delta\lambda_{max}$) diminishes with increasing chain length. While the gain in the red shift is relatively large between monomer **2** and dimer **7** ($\Delta\lambda_{max}$ = 59 nm), it is less pronounced between the larger homologues. Going from dimer **7** to trimer **9** the emission maximum is red-shifted by $\Delta\lambda_{max}$ = 41 nm, whereas $\Delta\lambda_{max}$ is only 11 nm between the highest analogues **9** and **10**.

All oligomeric model compounds exhibit smaller and more structured emission spectra compared to the corresponding absorption spectra. This is due to the reduced flexibility of the emitting chromophore leading to a stronger conjugation in the excited state.[19]

The quantum yields do not show an overall trend. Monomer **2** has the lowest quantum yields in this series (Φ = 0.08). Interestingly, the dimer **7** shows the largest quantum yield (Φ = 0.46), while the next higher oligomers **9** and **10** are exhibiting slightly lower quantum yields (Φ (**9**) = 0.36; Φ (**10**) = 0.43). The two longest representatives **9** and **10**, exhibit considerably stronger fluorescence in comparison with the corresponding oligo(3-hexylthiophene)s which show fluorescence quantum yields in the order of Φ = 0.30.

Table 1. Optical Properties of the Oligomeric Model Compounds 2, 7, 9, and 10

compound	λ_{max}^{abs} [a] [nm]	ε [a] [mol·L^{-1}·cm^{-1}]	ΔE_{opt} [b] [eV]	λ_{max}^{em} [nm]	Φ [c] [%]	Stokes shift [d] [cm^{-1} (eV)]
2	333 (*302*) [f]	18800 (*9800*) [f]	3.21 (*3.59*) [f]	410 [e] (*367*) [f]	8 (*2*) [f]	5640 (0.70) (*5865 (0.73)*) [f]
7	392 (*371*) [g]	40800 (*22800*) [g]	2.68 (*2.82*) [g]	**469**, 500 (*494*) [g]	46 (*13*) [g]	4188 (0.52) (*5723 (0.71)*) [g]
9	417 (*406*) [h]	54400 (*37000*) [h]	2.51 (*2.57*) [h]	**510**, 542 (*534*) [h]	36 (*29*) [h]	4373 (0.54) (*5904 (0.73)*) [h]
10	427 (*422*) [i]	78700 (*52300*) [i]	2.46 (*2.45*) [i]	**521**, 554 (*560*) [i]	43 (31) [i]	4225 (0.52) (*5840 (0.72)*) [i]

[a] $c = 5 \times 10^{-5}$ mol/L. Maxima are in bold. [b] Determined from the onset of the absorption at the lower energy band edge. [c] Quantum yields determined with respect to 9,10-diphenylantracene in air saturated solution; $c = 5 \cdot \times 10^{-7}$ mol/L.[17] [d] Stokes shifts measured as $\lambda_{max}^{em} - \lambda_{max}^{abs}$. [e] Excitation wavelength $\lambda^{ex} = 350$ nm, $\lambda^{ex} = 400$ nm. [f] For comparison are values for the parent nonfunctionalized dihexyl-bithiophene in parentheses. [g] Tetrahexyl-quaterthiophene. [h] Hexahexyl-sexithiophene. [i] Octahexyl-octithiophene.[18]

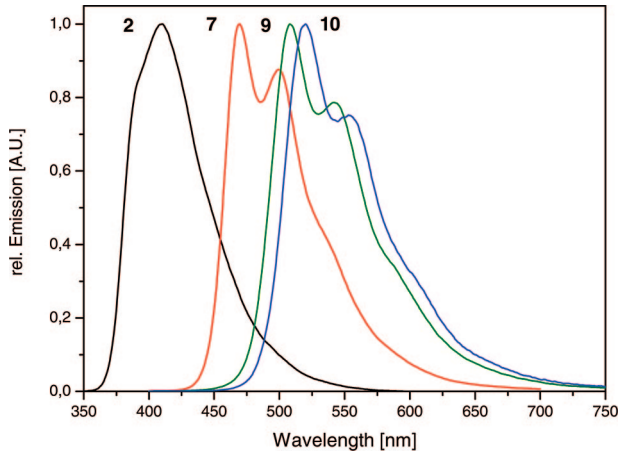

Figure 2. Normalized emission spectra of the oligomeric model compounds **2**, **7**, **9**, and **10** in chloroform ($\lambda^{ex} = 350$ nm for **2**, $\lambda^{ex} = 400$ nm for **7**, **9** and **10**).

For comparison the emission of the parent poly(hexylbithienylene ethynylene) exhibits a value of 535 nm with a shoulder at 575 nm and a fluorescence quantum yield of $\Phi = 0.34$.[1]

The Stokes shifts, measured as the difference between the absorption and the corresponding emission maxima, show constant values around 4200 cm^{-1} for the oligomers **7**, **9**, and **10**. The only exception is observed in the case of ethynyl-bithiophene **2** where the Stokes shift of 5600 cm^{-1} is considerably higher. In general, this is smaller in comparison with the corresponding oligo(3-hexylthiophene)s, exhibiting Stokes shifts of around 5900 cm^{-1}. The considerably smaller Stokes shifts are an indication that the ground state and the excited state are structurally more comparable in the case of the oligomeric model compounds **2**, **7**, **9**, and **10** rather than for the oligo(3-hexylthiophene)s. In the latter case a planar, quinoid structure can be postulated in the excited state, whereas a comparable quinoid structure cannot be formulated without interrupting the conjugation within the oligomers **2**, **7**, **9**, and **10**.

A correlation of the maximum absorption and emission energies versus the inverse number of atoms in the conjugated backbone (10 atoms per monomer unit of oligomeric series **2**, **7**, **9**, and **10** in comparison with 8 atoms per structurally comparable bithiophene units of the series of oligo(3-hexylthiophene)s) furnishes clear linear relationships with excellent correlation coefficients (Figure 3). A comparison to the corresponding correlation of the O3HTs demonstrates the influence of the triple bonds incorporated into the conjugated backbone of the oligomers **2**, **7**, **9**, and **10**. While in the case of the maximum absorption energies the correlations of both the oligomers **2**, **7**, **9**, and **10** and the corresponding oligo(3-hexylthiophene)s are in good agreement, a significant deviation can be observed in the case of the correlated emission maxima. In the latter case, the gap between both oligomeric series increases with elongation of the conjugated oligomer backbones, which can be expected from the different strongly pronounced Stokes shifts in these two series.

The oxidation potentials and the absolute HOMO levels of the oligomeric model compound series **2**, **7**, **9**, and **10** which have been determined by cyclic voltammetry are listed in Table 2.

Ethynyl-bithiophene **2** shows one irreversible oxidation at $E^\circ = 0.75$ V, while in the case of dimer **7** two quasireversible oxidations are observed at 0.56 and 0.77 V, respectively. With increasing length of the conjugated chain the oxidation potentials are shifted to more negative values and are becoming reversible (trimer **9**, $E^\circ = 0.50$ V, 0.62 V, 1.00 V; tetramer **10**, $E^\circ = 0.45$ V, 0.50 V, 0.77 V, 0.94 V). The progressive extension of the conjugated oligomer chain leads to an increased number of redox potentials which lie more closely together and are starting to overlap. While only one oxidation wave is observed for monomer **2**, two and three appear for dimer **7** and trimer **9**, respectively, leading to a final number of four redox waves in the case of tetramer **10**. Nevertheless, no reduction waves were observed down to potentials of −2.1 V versus ferrocene/ferricenium.

For comparison the cyclic voltammograms of the parent poly(hexylbithienylene ethynylene) exhibit two oxidation peaks at $E^\circ = 0.75$ V and $E^\circ = 1.10$ V, respectively, with a beginning of the oxidation at 0.60 V (Figure 4). In contrast, the parent polymer shows a reduction starting at −1.96 V leading to a HOMO of −5.20 eV, a LUMO of −2.84 eV, and an electrochemical band gap of 2.36 eV.[1]

The increasing number of oxidation waves observed for longer conjugated chains is due to the fact that the oxidation potentials are substantially lowered as a result of the larger delocalization of the corresponding radical cations throughout a bigger conjugated system. In this respect, each newly created radical gains more delocalization energy when the delocalized system increases, and at the same time the repulsive forces between several radical cation on the same chain are being reduced. As a result of these two effects the number of radical cations that can be generated at a certain oxidation potential increases when the delocalized system is enlarged.

(20) Pommerehne, J.; Vestweber, H.; Guss, W.; Mahrt, R. F.; Bässler, H.; Porsch, M.; Daub, J. *Adv. Mater.* **1995**, *7*, 551.
(21) Adams, N. R. *Electrochemistry at Solid Electrodes*; Marcel Dekker: New York, 1969, p 143.

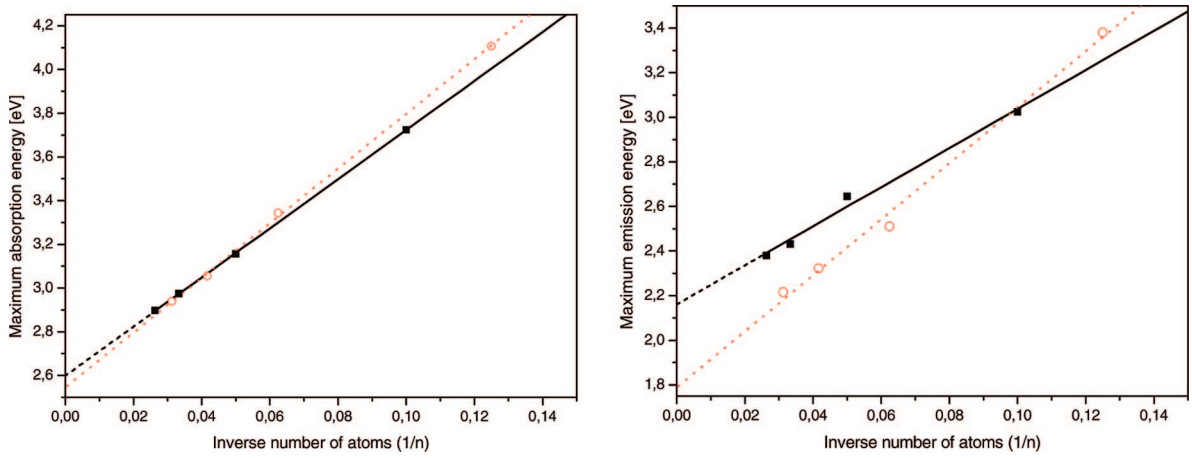

Figure 3. Maximum absorption (left) and emission (right) energies versus the inverse number of atoms in the conjugated backbone of the oligomeric series ([■] oligomeric series **2**, **7**, **9**, and **10**, [○] oligo(3-hexylthiophene)).[18]

Table 2. Electrochemical Properties of the Oligomeric Model Compounds 2, 7, 9, and 10

compound	$E°_{Ox1}$[a] [V]	$E°_{Ox2}$[a] [V]	$E°_{Ox3}$[a] [V]	$E°_{Ox4}$[a] [V]	HOMO[b] [eV]	LUMO[c] [eV]
2	0.75[d] (*0.83*)[e]	(*1.24*)[e]			−5.49 (*−5.52*)[e]	−2.28 (*−1.93*)[e]
7	0.56 (*0.43*)[f]	0.77 (*0.85*)[f]			−5.29 (*−5.16*)[f]	−2.61 (*−2.34*)[f]
9	0.50 (*0.30*)[g]	0.62 (*0.43*)[g]	1.00 (*1.20*)[g]		−5.22 (*−5.04*)[g]	−2.71 (*−2.47*)[g]
10	0.45 (*0.25*)[h]	0.50 (*0.34*)[h]	0.77 (*0.79*)[h]	0.94 (*1.21*)[h]	−5.19 (*−4.98*)[h]	−2.73 (*−2.53*)[h]

[a] In dichloromethane/nBu$_4$NPF$_6$ (0.1 M) vs Fc/Fc$^+$ at 100 mV/s. [b] Determined from the onset the oxidation waves and are related to the Fc/Fc$^+$ couple with a calculated absolute energy of −4.8 eV.[20] [c] LUMO levels are calculated via the optical band gaps. [d] Irreversible redox process, $E°$ determined at $I° = 0.855I_p$.[21] [e] For comparison values for the parent nonfunctionalized dihexyl-bithiophene in parentheses. [f] Tetrahexyl-quaterthiophene. [g] Hexahexyl-sexithiophene. [h] Octahexyl-octithiophene.[18]

A correlation of first oxidation potentials versus the inverse number of atoms in the conjugated backbone of the oligomers **2**, **7**, **9**, and **2** furnishes a clear linear relationship with an excellent correlation coefficient (Figure 5). This type of regression reveals a strong influence of the ethynylene moieties incorporated into the oligomer backbones on the electrochemical properties. In this respect, the corresponding oxidation potentials of the oligomers **2**, **7**, **9**, and **10** are more positive compared to the those of the oligo(3-hexylthiophene)s. The influence of the triple bonds becomes more and more pronounced with increasing length of the conjugated system, and accordingly, the slope of the regression is much steeper in the case of the oligo(3-hexylthiophene)s. In this respect, an infinite ideal polymer chain based on the oligomeric series **2**, **7**, **9**, and **10** should exhibit a first oxidation potential which is about 300 mV positively shifted with respect to an ideal poly(3-hexylthiophene).

An MO scheme of the oligomeric series **2**, **7**, **9**, and **10** is depicted in Figure 6, showing the HOMO levels which are determined from the onset of the first oxidation processes, while the LUMO levels are calculated from the corresponding optical band gaps. The elongation of the conjugated chain is accompanied by a progressive decrease of the HOMO energies from bithiophene **2** (−5.49 eV) to tetramer **10** (−5.19 eV). At the same time, the energetic levels of the corresponding LUMOs are decreasing in energy from **2** (−2.28 eV) to tetramer **10** (−2.73 eV), resulting in a gradual decline of the HOMO–LUMO band gap with increasing length of the conjugated oligomer backbone.

Conclusions

We synthesized a series of ethynylene-containing oligomers as new model compounds for a previously reported poly(hexylbithienylene ethynylene). This series has been built-up by palladium-catalyzed cross-coupling reactions from a monomer to a tetramer. The optical and electrochemical properties have been characterized and compared to a structurally related series of oligo(3-hexylthiophene)s, which in turn are excellent model compounds for the frequently used poly(3-hexylthiophene). Detailed investigations of the electronic properties of the series in solution clearly revealed that there is a systematic change in the spectral range of absorption, emission, fluorescence quantum yields, redox potentials, and energy gaps. In particular, the emission and oxidation behavior exhibits significant deviations from the analogous oligo(3-hexylthiophene)-series and, thus, emphasizes the interesting properties of the parent polymer.

Experimental Section

General Procedures. ^{1}H NMR spectra were recorded in $CDCl_3$ on a Bruker AMX 400 at 400 MHz. ^{13}C NMR spectra were recorded in $CDCl_3$ on a Bruker AMX 400 at 100 MHz. Chemical shifts are denoted in δ unit (ppm) and were referenced to internal tetramethylsilane (0.0 ppm). The splitting patterns are designated as follows: s (singlet), d (doublet), t (triplet), quin (quintet), and m (multiplet), and the assignments are *Th* (thiophene) for ^{1}H NMR. Mass spectra were recorded with a Varian Saturn 2000 GC-MS and with a MALDI-TOF MS Bruker Reflex 2 (dithranol as the matrix). Elemental analyses were performed on an Elementar Vario EL. Melting points were determined with a Büchi B-545 melting point apparatus and are not corrected. Gas chromatography was carried out using a Varian CP-3800 gas chromatograph. HPCL analyses were performed on a Shimadsu SCL-10A equipped with a SPD-M10A photodiode array detector and a SC-10A solvent delivery system using a *LiChrosphor* column (Silica 60, 5 μm, Merck). Thin-layer chromatography was carried out on Silica Gel 60 F_{254} aluminum plates (Merck). Developed plates were dried and

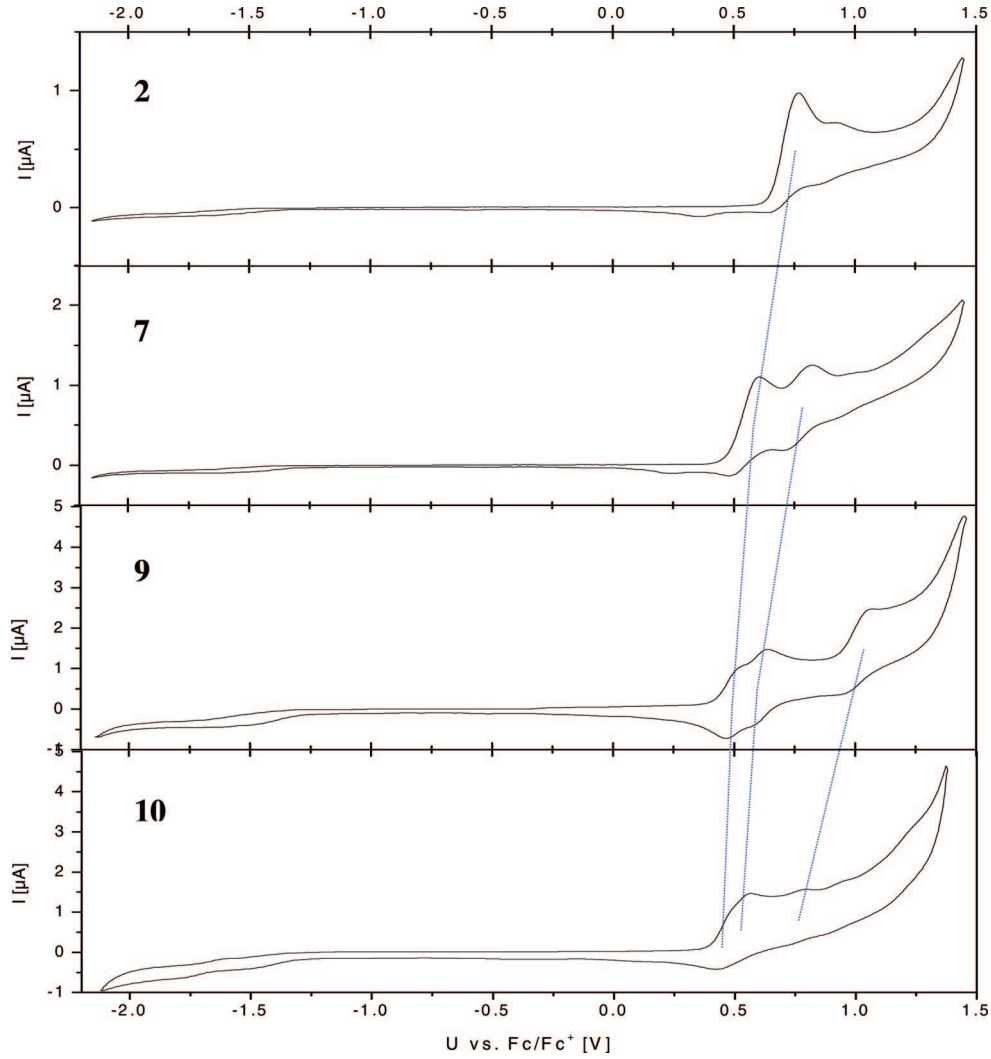

Figure 4. Cyclic voltammograms of **2**, **7**, **9**, and **10** in dichloromethane/*n*-Bu_4NPF_6 (0.1 M) versus Fc/Fc^+ at 100 mV/s.

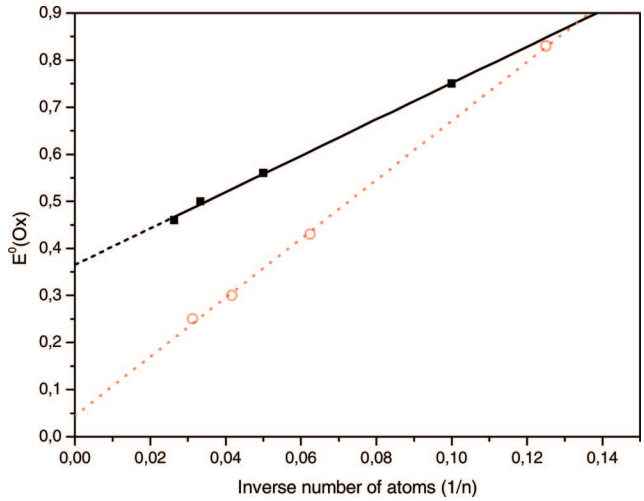

Figure 5. First oxidation potentials versus the inverse number of atoms in the conjugated backbone of the oligomeric series ([■] oligomeric series **2**, **7**, **9**, and **10**, [○] oligo(3-hexylthiophene)[18]).

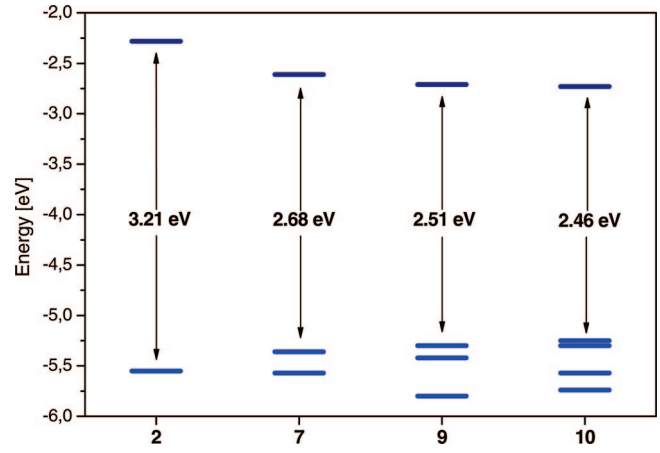

Figure 6. MO scheme of the oligomeric model compounds **2**, **7**, **9**, and **10**.

examined under a UV lamp. Preparative column chromatography was carried out on glass columns of different sizes packed with silica gel Merck 60 (40–63 μm). UV–vis spectra were taken on a Perkin-Elmer Lambda 19 in 1 cm cuvettes. Thin uniform films for solid-state spectra were obtained on a POLOS wafer spinner from a toluene solution (20 mg/mL) at 5000 rpm onto a glass substrate. Fluorescence spectra were measured with a Perkin-Elmer LS 55 in 1 cm cuvettes. Fluorescence quantum yields were determined with respect to 9,10-diphenylanthracene ($\Phi = 0.9$ in hexane[17]). Cyclic voltammetry experiments were performed with a computer-controlled EG&G PAR 273 potentiostat in a three-electrode single-compartment cell (5 mL). The platinum working electrode consisted of a platinum wire sealed in a soft glass tube with a surface of *A*

$= 0.785$ mm^2, which was polished down to 0.5 μm with Buehler polishing paste prior to use in order to obtain reproducible surfaces. The counter electrode consisted of a platinum wire, and the reference electrode was an Ag/AgCl secondary electrode. All potentials were internally referenced to the ferrocene/ferricenium couple.[20] For the measurements concentrations of 10^{-3} mol/L of the electroactive species were used in freshly distilled and deairated dichloromethane (*Lichrosolv*, Merck) and 0.1 M tetrabutylammonium hexafluorophosphate (nBu$_4$NPF$_6$, Fluka) which was twice recrystallized from ethanol and dried under vacuum prior to use. Solvents and reagents were purified and dried by the usual methods prior to use and typically used under inert gas atmosphere. The following starting materials were purchased and used without further purification: *n*-butyllithium (*n*-BuLi, Merck) was a 1.6 M solution in *n*-hexane, iodine (Merck), dichloro-diisopropyl-silan (Fluka), benzylic alcohol (Merck), ethynyl-trimethyl-silan (Fluka), *n*-tetrabutylammonium fluoride (Merck), and Pd(PPh$_3$)$_2$Cl$_2$ (Merck). Pd(PPh$_3$)$_4$[22] was prepared according to a literature procedure.

Synthesis. *(4,3′-Dihexyl-2,2′-bithienyl-5-ylethynyl)trimethylsilane (**2**).* **1** (827 mg, 2 mmol), ethynyl-triisopropyl-silane (437 mg, 2.4 mmol), CuI (38 mg, 0.2 mmol), and Pd(PPh$_3$)$_4$ (116 mg, 0.1 mmol) were added to 15 mL of piperidine. After the reaction mixture was carefully degassed it was stirred at 90 °C for 3 h. After the reaction was completed the mixture was poured into water (50 mL) and was acidified with concentrated hydrochloric acid (pH = 1). The organic layer was taken off while the water phase was extracted with dichloromethane. The combined organic phases were dried with magnesium sulfate, and the solvent was removed by rotary evaporation. The crude product was purified by column chromatography (SiO$_2$/petrol ether) to give **2** (930 mg, 90%) as a yellow, viscous oil. ^{1}H NMR (400 MHz, CDCl$_3$): $\delta = 7.14$ (d, $J = 5.2$ Hz, 1H, 5′-*H*), 6.91 (d, $J = 5.2$ Hz, 1H, 4′-*H*), 6.84 (s, 1H, 3-*H*), 2.74 (t, $J = 7.8$ Hz, 2H, α′-*H*), 2.69 (t, $J = 7.7$ Hz, 2H, α-*H*), 1.66–1.58 (m, 4H, β,β′-*H*), 1.45–1.25 (m, 12H, -C*H*$_2$-), 1.15–1.10 (m, 21H, Si-C*H*-(CH$_3$)$_2$, Si-CH-(C*H*$_3$)$_2$), 0.88 (t, $J = 6.7$ Hz, 6H, -C*H*$_3$). ^{13}C NMR (100 MHz, CDCl$_3$): $\delta = 149.01$, 140.02, 135.97, 130.40, 130.09, 126.71, 123.87, 118.32, 98.97, 98.34, 31.68, 31.65, 30.30, 29.85, 29.25, 29.19, 29.08, 22.62, 18.70, 14.08, 11.33. MS (EI): m/z [M$^+$] = 515. Anal. Calcd for C$_{31}$H$_{31}$S$_2$Si: C, 72.31; H, 9.79; S, 12.45. Found: C, 72.53; H, 9.98; S, 12.74.

*(4,3′-Dihexyl-5′-iodo-2,2′-bithien-5-ylethynyl)triisopropyl-silane (**3**).* A suspension of **2** (2.06 g, 4.0 mmol) and mercury caproate (1.72 g, 4.0 mmol) in 15 mL of dry chloroform was stirred at room temperature for 24 h. After the mercury compound was completely dissolved, iodine (1.07 g, 4.4 mmol) was added, and the mixture was stirred for another hour. Next the precipitate was filtered off, and the solvent was removed by rotary evaporation. The crude product was purified by column chromatography (SiO$_2$/petrol ether) to give **3** (2.23 g, 87%) as a yellow, viscous oil. ^{1}H NMR (400 MHz, CDCl$_3$): $\delta = 7.04$ (s, 1H, 4′-*H*), 6.78 (s, 1H, 3-*H*), 2.71–2.65 (m, 4H, α,α′-*H*), 1.66–1.56 (m, 4H, β,β′-*H*), 1.40–1.25 (m, 12H, -C*H*$_2$-), 1.15–1.10 (m, 21H, Si-C*H*-(CH$_3$)$_2$, Si-CH-(C*H*$_3$)$_2$), 0.88 (t, $J = 6.7$ Hz, 6H, -C*H*$_3$). ^{13}C NMR (100 MHz, CDCl$_3$): $\delta = 148.99$, 141.79, 139.81, 136.39, 134.39, 127.09, 118.92, 98.90, 97.15, 71.83, 31.66, 31.59, 30.51, 30.26, 29.80, 29.09, 29.06, 28.90, 22.61, 22.58, 18.68, 14.07, 11.31. MS (EI): m/z [M$^+$] = 640. Anal. Calcd for C$_{31}$H$_{30}$IS$_2$Si: C, 58.10; H, 7.71; S, 10.01. Found: C, 57.93; H, 7.51; S, 9.94.

*Chloro(4,3′-dihexyl-2,2′-bithien-5-yl)diisopropyl-silane (**4**).* **1** (1.0 g, 2.42 mmol) was dissolved in 12 mL of THF. At −80 °C *n*-butyllithium (1.54 mL, 2.46 mmol) was added dropwise, and the resulting solution was stirred for 1 h at −80 °C. After addition of dichloro-diisopropyl-silan (0.67 g, 3.63 mmol) the solution was allowed to warm up to room temperature and stirred for another hour. Next, the solvent was removed by rotary evaporation, and the residue was dissolved in petrol ether. The white precipitate was filtered off, and the solvent was evaporated. The excess of dichloro-diisopropyl-silan was removed in vacuum. **4** was obtained as a pale yellow viscous liquid (1.17 g, quantitative yield) and was used without further purification. ^{1}H NMR (400 MHz, CDCl$_3$): $\delta = 7.18$ (d, $J = 5.2$ Hz, 1H, 5′-*H*), 7.11 (s, 1H, 3-*H*), 6.93 (d, $J = 5.2$ Hz, 1H, 4′-*H*), 2.79 (t, $J = 7.8$ Hz, 2H, α′-*H*), 2.73 (t, $J = 8.0$ Hz, 2H, α-*H*), 1.71–1.61 (m, 4H, β,β′-*H*), 1.50–1.30 (m, 14H,-C*H*$_2$-, Si-C*H*-(CH$_3$)$_2$), 1.17 (d, $J = 7.2$ Hz, 6H, Si-CH-(C*H*$_3$)$_2$), 1.12 (d, $J = 7.3$ Hz, 6H, Si-CH-(C*H*$_3$)$_2$), 0.94–0.89 (m, 6H, -C*H*$_3$). ^{13}C NMR (100 MHz, CDCl$_3$): $\delta = 152.54$, 142.13, 139.77, 130.51, 130.10, 129.06, 124.92, 123.69, 31.92, 31.73, 31.63, 31.47, 30.59, 29.42, 29.31, 29.19, 22.63, 17.34, 17.04, 15.68, 14.06. MS (EI): m/z [M$^+$] = 483.

*Benzyloxy(4,3′-dihexyl-2,2′-bithien-5-yl)diisopropyl-silane (**5**).* **4** (2.90 g, 6 mmol) was added to a solution of benzylic alcohol (0.97 g, 9 mmol) and imidazole (1.02 g, 15 mmol) in 50 mL of dry DMF. After stirring for 24 h at room temperature the reaction mixture was poured into 10 mL of water, and the water phase was extracted with petrol ether. The organic phase was dried with magnesium sulfate before the solvent was removed by rotary evaporation. The crude product was purified by column chromatography (SiO$_2$/petrol ether: dichloromethane [10:1]) to give **5** (2.6 g, 78%) as a yellow viscous liquid. ^{1}H NMR (400 MHz, CDCl$_3$): $\delta = 7.43$–7.34 (m, 4H, Ph-2*H*, 3*H*, 5*H*, 6*H*), 7.28 (m, 1H, Ph-4*H*), 7.17 (d, $J = 5.2$ Hz, 1H, 5′-*H*), 7.13 (s, 1H, 3-*H*), 6.94 (d, $J = 5.2$ Hz, 1H, 4′-*H*), 4.94 (s, 2H, Ph-C*H*$_2$-), 2.80 (t, $J = 7.8$ Hz, 2H, α′-*H*), 2.69 (t, $J = 8.1$ Hz, 2H, α-*H*), 1.70–1.60 (m, 4H, β,β′-*H*), 1.46–1.22 (m, 14H,-C*H*$_2$-, Si-C*H*-(CH$_3$)$_2$), 1.20–1.13 (m, 12H, Si-CH-(C*H*$_3$)$_2$), 0.95–0.85 (m, 6H, -C*H*$_3$). ^{13}C NMR (100 MHz, CDCl$_3$): $\delta = 152.31$, 141.30, 141.00, 139.40, 130.98, 130.08, 128.70, 128.17, 128.15, 126.96, 126.89, 125.93, 123.34, 65.56, 31.77, 31.69, 31.66, 31.60, 30.63, 29.51, 29.35, 29.23, 22.64, 17.76, 17.62, 14.06, 13.99. MS (MALDI-TOF): m/z [M + H$^+$] = 555. Anal. Calcd for C$_{33}$H$_{50}$OS$_2$Si: C, 71.42; H, 9.08; S, 11.56. Found: C, 71.49; H, 9.17; S, 11.62.

*Benzyloxy(5′-iodo-4,3′-dihexyl-2,2′-bithien-5-yl)diisopropyl-silane (**6**).* **5** (1.1 g, 2 mmol) was dissolved in 20 mL of dry dichloromethane. After addition of mercury caproate (870 mg, 2.02 mmol) the resulting suspension was stirred for 24 h until the mercury compound was completely dissolved. After addition of iodine (558 mg, 2.2 mmol) the reaction mixture was stirred for another 2 h. Then the solution was filtered over basic aluminum oxide with petrol ether as the eluent. After the solvent was taken off **6** was obtained as a yellow viscous liquid (1.3 g, 95%). ^{1}H NMR (400 MHz, CDCl$_3$): $\delta = 7.43$–7.34 (m, 4H, Ph-2*H*, 3*H*, 5*H*, 6*H*), 7.28 (m, 1H, *Ph*-4*H*), 7.07 (s, 1H, 3-*H*), 7.05 (s, 1H, 4′-*H*), 4.93 (s, 2H, Ph-C*H*$_2$-), 2.74 (t, $J = 7.9$ Hz, 2H, α′-*H*), 2.68 (t, $J = 8.1$ Hz, 2H, α-*H*), 1.67–1.55 (m, 4H, β,β′-*H*), 1.40–1.20 (m, 14H,-C*H*$_2$-, Si-C*H*-(CH$_3$)$_2$), 1.19–1.13 (m, 12H, Si-CH-(C*H*$_3$)$_2$), 0.95–0.85 (m, 6H, -C*H*$_3$). ^{13}C NMR (100 MHz, CDCl$_3$): $\delta = 152.19$, 141.07, 140.07, 139.76, 137.01, 128.94, 128.08, 127.71, 126.82, 125.84, 71.15, 65.50, 31.64, 31.53, 31.48, 31.45, 30.43, 29.36, 29.01, 28.97, 28.89, 22.49, 17.63, 14.49, 13.94, 13.87. MS (MALDI-TOF): m/z [M + H$^+$] = 681. Anal. Calcd for C$_{33}$H$_{49}$IOS$_2$Si: C, 58.21; H, 7.25; S, 9.42. Found: C, 58.35; H, 7.31; S, 9.63.

*({5′-[(3,4′-Dihexyl-2,2′-bithien-5-yl)ethynyl]-3,4′-dihexyl-2,2′-bithien-5-yl}ethynyl)triisopropyl-silane (**7**).* **2** (515 mg, 1 mmol) was dissolved in 5 mL of THF, and cesium fluoride (755 mg, 5 mmol) dissolved in 1 mL of methanol was added. The resulting solution was degassed and was stirred for 2 h at 70 °C. After the reaction

(22) Coutts, I. C. G.; Goldschmidt, H. R.; Musgrave, O. C. *J. Chem. Soc.* **1970**, 488.

was completed the mixture was poured into water, and the organic layer was taken off while the water phase was extracted with dichloromethane. The combined organic phases were dried with magnesium sulfate, and the solvent was removed by rotary evaporation. The crude product was filtrated over a short column chromatography (SiO_2/petrol ether) to give **2a** as a yellow, viscous oil and subsequently was added to a mixture of **3** (513 mg, 0.8 mmol), CuI (15 mg, 0.08 mmol), and $Pd(PPh_3)_2Cl_2$ (28 mg, 0.04 mmol) dissolved in 4 mL of piperidine. After the resulting yellow solution was carefully degassed it was stirred at 60 °C for 1 h. When the reaction was completed the mixture was poured into water and was acidified with concentrated hydrochloric acid (pH = 1). The organic layer was taken off while the water phase was extracted with dichloromethane. The combined organic phases were dried with magnesium sulfate, and the solvent was removed by rotary evaporation. The crude product was purified by column chromatography (SiO_2/petrol ether) to give **7** (570 mg, 82%) as a yellow, viscous oil. ^{1}H NMR (400 MHz, $CDCl_3$): δ = 7.16 (d, J = 5.3 Hz, 1H, 5‴-*H*); 7.06 (s, 1H, 4′-*H*), 6.92 (d, J = 5.3 Hz, 1H, 4‴-*H*); 6.90 (s, 1H, 3-*H*), 6.87 (s, 1H, 3″-*H*), 2.79–2.67 (m, 8H, α-*H*), 1.72–1.60 (m, 8H, *β*-*H*), 1.45–1.30 (m, 24H, -CH_2-), 1.14 (s, 21H, Si-C*H*-$(CH_3)_2$, Si-CH-$(CH_3)_2$), 0.90–0.80 (m, 12H, -CH_3). ^{13}C NMR (100 MHz, $CDCl_3$): δ = 149.22, 148.76, 140.31, 140.11, 137.18, 135.15, 134.80, 132.58, 130.51, 130.35, 127.15, 126.97, 124.12, 121.26, 119.08, 117.62, 99.15, 98.97, 89.42, 87.17, 31.82, 31.79, 30.78, 30.50, 30.41, 30.30, 29.97, 29.86, 29.53, 29.44, 29.39, 29.28, 29.22, 29.09, 22.78, 22.76, 22.75, 18.85, 14.27, 14.21, 11.50. MS (MALDI-TOF): m/z [M + H$^+$] = 871. Anal. Calcd for $C_{53}H_{78}S_4Si$: C, 73.04; H, 9.02; S, 14.72. Found: C, 73.23; H, 9.11; S, 15.01.

*5′-({5′-[(3,4′-Dihexyl-2,2′-bithien-5′-iodo-5-yl)ethynyl]-3,4′-dihexyl-2,2′-bithien-5-yl}ethynyl)triisopropyl-silane (**8**).* A suspension of **7** (500 mg, 0.57 mmol) and mercury caproate (247 mg, 0.57 mmol) in 5 mL of dry chloroform was stirred at room temperature for 24 h. After the mercury compound was completely dissolved, iodine (160 mg, 0.64 mmol) was added and the mixture was stirred for another hour. Next the precipitate was filtered off, and the solvent was removed by rotary evaporation. The crude product was purified by column chromatography (SiO_2/petrol ether) to give **8** (460 mg, 81%) as an orange, viscous oil. ^{1}H NMR (400 MHz, $CDCl_3$): δ = 7.07 (s, 1H, 4‴-*H*); 7.06 (s, 1H, 4′-*H*), 6.88 (s, 1H, 3-*H*), 6.84 (s, 1H, 3″-*H*), 2.76–2.69 (m, 8H, α-*H*), 1.72–1.58 (m, 8H, *β*-*H*), 1.40–1.25 (m, 24H, -CH_2-), 1.15 (s, 21H, Si-C*H*-$(CH_3)_2$, Si-CH-$(CH_3)_2$), 0.95–0.80 (m, 12H, -CH_3). ^{13}C NMR (100 MHz, $CDCl_3$): δ = 149.22, 148.71, 142.03, 140.11, 140.06, 136.51, 135.57, 135.10, 134.91, 132.73, 127.31, 127.17, 121.09, 119.13, 118.25, 99.19, 98.95, 89.85, 86.89, 72.14, 31.82, 31.77, 30.70, 30.50, 30.41, 30.27, 29.97, 29.81, 29.44, 29.31, 29.28, 29.22, 29.20, 29.07, 22.77, 22.75, 18.85, 14.26, 14.22, 11.50. MS (MALDI-TOF): m/z [M + H$^+$] = 997. Anal. Calcd for $C_{53}H_{77}IS_4Si$: C, 63.82; H, 7.78; S, 12.86. Found: C, 64.02; H, 7.99; S, 12.81.

*5′-{5′-[(3,4′-Dihexyl-2,2′-bithien-5-yl)ethynyl]-5′-[(3,4′-dihexyl-2,2′-bithien-5-yl)ethynyl]}-[3,4′-dihexyl-2,2′-bithien-5-yl]ethynyl)triisopropyl-silane (**9**).* **8** (450 mg, 0.45 mmol), **2a** (237 mg, 0.55 mmol), CuI (9 mg, 0.045 mmol), and $Pd(PPh_3)_2Cl_2$ (16 mg, 23 μmol) were dissolved in 3 mL of piperidine. After the resulting orange solution was carefully degassed it was stirred at 60 °C for 1 h. When the reaction was completed the mixture was poured into water and was acidified with concentrated hydrochloric acid (pH = 1). The organic layer was taken off while the water phase was extracted with dichloromethane. The combined organic phases were dried with magnesium sulfate, and the solvent was removed by rotary evaporation. The crude product was purified by column chromatography (SiO_2/petrol ether:dichloromethane [20:1]) to give **9** (250 mg, 45%) as an orange-red, viscous oil. ^{1}H NMR (400 MHz, $CDCl_3$): δ = 7.17 (d, J = 5.0 Hz, 1H, 4⁗′-*H*), 7.07 (s, 2H, 4′,4‴-*H*), 6.93 (s, 1H, 3-*H*), 6.92 (d, J = 5.0 Hz, 1H, 5⁗′-*H*), 6.90 (s, 1H, 3″-*H*), 6.88 (s, 1H, 3⁗-*H*), 2.80–2.68 (m, 12H, α-*H*), 1.75–1.60 (m, 12H, *β*-*H*), 1.45–1.25 (m, 36H, -CH_2-), 1.15 (s, 21H, Si-C*H*-$(CH_3)_2$, Si-CH-$(CH_3)_2$), 0.95–0.85 (m, 18H, -CH_3). ^{13}C NMR (100 MHz, $CDCl_3$): δ = 149.23, 148.81, 148.78, 140.32, 140.22, 140.13, 137.22, 136.17, 135.11, 134.91, 134.88, 132.73, 132.50, 130.49, 130.35, 127.21, 127.17, 126.96, 124.13, 121.35, 121.10, 119.12, 118.21, 117.59, 99.19, 98.95, 89.93, 89.42, 87.83, 87.04, 31.81, 31.78, 30.77, 30.54, 30.50, 30.41, 30.31, 30.28, 29.97, 29.86, 29.82, 29.57, 29.54, 29.43, 29.39, 29.35, 29.28, 29.21, 29.08, 22.78, 22.76, 22.74, 18.84, 14.27, 14.23, 14.21, 11.50. MS (MALDI-TOF): m/z [M + H$^+$] = 1227. Anal. Calcd for $C_{75}H_{106}S_6Si$: C, 73.35; H, 8.70; S, 15.66. Found: C, 73.54; H, 8.91; S, 16.76.

*5-[(4,3′-Dihexyl-2,2′-bithien-5-yl)ethynyl]-5′-({5′-[(3,4′-dihexyl-2,2′-bithien-5-yl)ethynyl]-3,4′-dihexyl-2,2′-bithien-5-yl}ethynyl)-3,4′-dihexyl-2,2′-bithiophene (**10**).* **9** (200 mg, 0.16 mmol) was dissolved in 5 mL of THF, and cesium fluoride (121 mg, 0.8 mmol) dissolved in 0.5 mL of methanol was added. The resulting solution was stirred for 2 h at 70 °C. After the reaction was completed the mixture was poured into water and the organic layer was taken off while the water phase was extracted with dichloromethane. The combined organic phases were washed with water three times and were dried with $MgSO_4$ before the solvent was removed by rotary evaporation. The residual orange-red oil **20** was dissolved in 3 mL of piperidine prior to the addition of **6** (129 mg, 0.19 mmol), CuI (3 mg, 16 μmol), and $Pd(PPh_3)_4$ (9 mg, 8 μmol). Next, the mixture was degassed and was stirred at 60 °C. After 1 h *n*-tetrabutylammonium fluoride (252 mg, 0.8 mmol) was added to the reaction mixture, which then was heated up to 80 °C. After the mixture was stirred for another hour it was poured onto water, and it was extracted with dichloromethane. The organic phase was dried with magnesium sulfate, and the solvent was taken off. The crude product was purified by column chromatography (SiO_2/petrol ether:dichloromethane [20:1] to give **10** (150 mg, 67%) as a red, viscous oil which crystallized to a red solid overnight. Mp: 40–41 °C. ^{1}H NMR (400 MHz, $CDCl_3$): δ = 7.17 (d, J = 5.0 Hz, 1H, 4⁗′-*H*), 7.09–7.07 (m, 3H, 4′,4‴,4⁗′-*H*), 7.00 (d, J = 1.3 Hz, 1H, 5-*H*), 6.97–6.95 (m, 2H, 3,3⁗′-*H*), 6.94 (d, J = 5.0 Hz, 1H, 5⁗′-*H*), 6.93–6.91 (m, 2H, 3″,3⁗-*H*), 2.81–2.73 (m, 14H, α′-α⁗′-*H*), 2.63 (t, J = 7.7 Hz, 2H, α-*H*), 1.75–1.60 (m, 16H, *β*-*H*), 1.45–1.25 (m, 48H, -CH_2), 0.95–0.85 (m, 24H, -CH_3). ^{13}C NMR (100 MHz, $CDCl_3$): δ = 148.81, 148.76, 148.65, 143.88, 140.28, 140.20, 140.18, 139.44, 137.21, 136.17, 135.95, 135.12, 134.96, 134.86, 134.83, 133.49, 132.68, 132.48, 130.47, 130.33, 127.75, 127.20, 127.18, 126.93, 124.11, 121.33, 121.12, 120.63, 120.55, 118.39, 118.18, 117.57, 90.09, 89.09, 89.42, 87.33, 87.16, 86.59, 31.82, 31.79, 31.76, 31.01, 30.75, 30.59, 30.51, 30.30, 30.27, 29.84, 29.79, 29.55, 29.52, 29.38, 29.33, 29.30, 29.13, 29.07, 22.77, 22.75, 14.26, 14.22. MS (MALDI-TOF): m/z [M + H$^+$] = 1403. Anal. Calcd for $C_{86}H_{114}S_8$: C, 73.55; H, 8.18; S, 18.27. Found: C, 73.31; H, 8.03; S, 18.15.

Acknowledgment. We would like to thank the German Ministry for Education and Research (BMBF Netzwerk "Polymere Solarzellen") for funding. J.C. would like to thank the "Fonds der Chemischen Industrie" and the German Ministry for Education and Research (BMBF) for a Kekulé-Grant.

CM703606H